ELSEVIER

Journal of Photochemistry and Photobiology A: Chemistry 135 (2000) 221–228

Journal of Photochemistry and Photobiology A:Chemistry

www.elsevier.nl/locate/jphotochem

Primary mechanism in the degradation of 4-octylphenol photoinduced by Fe(III) in water–acetonitrile solution

Nathalie Brand, Gilles Mailhot, Mohamed Sarakha, Michèle Bolte*

Laboratoire de Photochimie Moléculaire et Macromoléculaire, UMR CNRS 6505, Université Blaise Pascal, avenue des Landais, 63177 Aubière cedex, France

Received 16 March 1999; received in revised form 6 March 2000; accepted 17 April 2000

Abstract

The degradation of 4-octylphenol (4-OP), a toxic and persistent product in the environment, photoinduced by Fe(III) has been investigated in water/acetonitrile solution (95/5 by volume). The initial rate of 4-OP degradation depends on the irradiation wavelength and on the initial concentration of $Fe(OH)^{2+}$, the monomeric species present in our experimental conditions. Several photoproducts have been identified among them 4-(1,1,3,3-tetramethylbutyl)pyrocatechol. The formation of octylphenoxyl radical was observed by fast kinetics as a result of the quenching reaction between Fe(III) species in the excited state and 4-OP. For longer irradiation times, regeneration of the monomeric species, $Fe(OH)^{2+}$, was suggested due to Fe(II) reoxidation by radicals.

Keywords: Iron(III); 4-Octylphenol; Photodegradation; Hydroxyl radical

1. Introduction

Alkylphenol ethoxylates are among the most widely used group of surfactants. Worldwide, ca. 500,000 t are produced annually for use in different industrial fields and more particularly in detergents [1]. Alkylphenol ethoxylates have received a special attention in recent years because of their incomplete elimination during sewage treatment and the detection of biorefractory degradation intermediates in sludge, secondary effluents and rivers receiving such effluents [2]. Among the most common residues detected are the alkylphenols (AP) [2–5]. These compounds are also applied as emulsifiers in pesticide formulations. As a result, AP are found in large amounts in the aquatic environment. The high aquatic toxicity of these chemicals is now clearly established (e.g. LC_{50} for shrimp and salmon between 0.13 and 0.3 mg of nonylphenol per litter) [6].

Among the different abiotic degradation processes, solar irradiation is one of the factors responsible for pollutant degradation in the surface waters. When the pollutant does not absorb solar light, its transformation may be photoinduced by Fe(III) aquo-complexes. In the presence of Fe(III), two different photoprocesses can be observed depending on the nature of the pollutant. (i) If the pollutant is a complexing agent, such as nitrilotriacetic acid (NTA) [7], ethylenediaminetetra-acetic acid (EDTA) [8] or ethylenediaminetetra-methylenephosphonic acid (EDTMP) [9], a complex between the pollutant and Fe(III) which absorbs in the near UV–VIS spectral region is formed. In this case an intramolecular photoredox process leading to the degradation of the pollutants is observed. (ii) If Fe(III) is not complexed by the pollutant, Fe(III) aquo-complexes can absorb the solar light and undergo a photoredox process giving rise to Fe(II) and hydroxyl radicals [10,11]. Among the Fe(III) aquo-complexes, $Fe(OH)^{2+}$ (which refers to $Fe(OH)(H_2O)_5{}^{2+}$) is photolysed with the highest quantum yield [11], according to the following reaction:

$$Fe(OH)^{2+} \xrightarrow{h\nu} Fe^{2+} + {}^{\bullet}OH$$

In pure water the pollutant is attacked by $^{\bullet}OH$ radicals, strong oxidizing agents, leading to its degradation. We have previously investigated the degradation of pollutants photoinduced by Fe(III) [12–15]. In the particular case of 2,6-dimethylphenol (DMP), a quenching reaction between Fe(III) in the excited state and DMP was observed together with the formation of $^{\bullet}OH$ radicals [12]. In a previous study, concerning the degradation of a mixture of octylphenol ethoxylates photoinduced in pure water by Fe(III), we pointed out that octylphenol was among the intermediate photoproducts and was totally degraded [15]: the degradation photoinduced by Fe(III) of AP, toxics persistent in the environment, appears to be an interesting process for the AP removal in aqueous solution.

* Corresponding author. Fax: +33-4-73-40-77-00.
E-mail address: michele.bolte@univ-bpclermont.fr (M. Bolte)

1010-6030/00/$ – see front matter
PII: S1010-6030(00)00299-9

In the present study, we are more particularly interested in the primary mechanism of the 4-(1,1,3,3-tetramethylbutyl) phenol degradation photoinduced by Fe(III) in water/acetonitrile solution. Several photoproducts have been identified and a proposed degradation mechanism is given.

2. Experimental details

2.1. Reagents and solutions

4-(1,1,3,3-tetramethylbutyl)phenol (97%) and 1,4-benzoquinone (98%) were Aldrich products. 4-hydroxyacetophenone (98%) was purchased from Acros and used as received. Throughout this paper, 4-OP (4-octylphenol) will be used as an abbreviation of 4-(1,1,3,3-tetramethylbutyl)phenol. Ferric perchlorate nonahydrate [$Fe(ClO_4)_3$, $9H_2O$; 97%] was a Fluka product kept in a desiccator. The Fe(III) solutions for the studies were prepared by diluting stock solution [2.0×10^{-3} mol l^{-1} in $Fe(ClO_4)_3$, $9H_2O$] to the appropriate Fe(III) concentration. Acetonitrile (HPLC grade) and 2-propanol (HPLC grade Chromanorm >99.7%) were purchased from Carlo–Erba and Prolabo, respectively. Azidopentaammine cobalt(III), $[Co(NH_3)_5N_3]^{2+}$, was synthesized using the procedure described by Linhard and Flygare [16]. All solutions were prepared with water purified by a Millipore Milli-Q device. pH measurements were carried out with an ORION pH-meter to ±0.01 pH unit. The ionic strength was not controlled. The deaeration of the solutions was performed by six cycles of freeze–vaccum–thaw on a vacuum line.

2.2. Apparatus

HPLC experiments were carried out using a Waters 540 chromatograph equipped with a Waters 996 photodiode array detector. The flow rate was 1 ml min^{-1}. The reversed-phase column was a Touzard and Matignon Kromasil C_{18} (250 mm long×4.6 mm i.d., particle diameter 5 μm) and the eluent was a mixture of acetonitrile/water (75/25 by volume). The photoproducts were separated using a Gilson preparative HPLC set-up equipped with a Waters model 490 detector. The flow rate was 5 ml min^{-1} and the reversed-phase column was a Rainin Microsorb C_{18} (50 mm long×21.4 mm i.d., p.d. 3 μm). The eluent was a mixture of methanol/water (75/25 by volume). Liquid chromatography/negative electrospray/mass spectra (LC/ES/MS) were obtained from 'Service Central d'Analyse', CNRS (Vernaison, France). The flow rate was 0.2 ml min^{-1} and the reversed-phase column was a Hewlett–Packard ODS Hypersil (250 mm long×2 mm i.d., p.d. 5 μm). The eluent was a mixture of acetonitrile/water (50/50 by volume).

UV–VIS spectra were recorded on a CARY 3 double beam spectrophotometer. ^1H NMR spectra were recorded on a BRUKER AC 400 MHz Fourier transform spectrometer.

Monochromatic irradiations at 296, 313, 334, and 365 nm were carried out with a high-pressure mercury lamp (Ushio USH-200DP) equipped with a grating monochromator (Baush and Lomb). The beam was parallel and the reactor was a quartz cell of 2 cm path length. The light intensity was measured by ferrioxalate actinometry [17] [$I_{0(365\,nm)}\approx 2.2\times10^{15}$ photons s^{-1} cm^{-2}; $I_{0(334\,nm)}\approx6.0\times10^{14}$ photons s^{-1} cm^{-2}; $I_{0(313\,nm)}\approx1.2\times10^{15}$ photons s^{-1} cm^{-2}; $I_{0(296\,nm)}\approx5.9\times10^{14}$ photons s^{-1} cm^{-2}]. A second irradiation set-up used to monitor the photoproducts formation was an elliptical stainless-steel cylinder. A high-pressure mercury lamp (Philips HPW 125 W), the emission of which at 365 nm was selected by an inner filter, was located at a focal axis of the elliptical cylinder. The reactor, a water-jacketed Pyrex tube (diameter=2.8 cm), was centred at the other focal axis. The reaction medium was well stirred. The unit delivered an intensity $I_0\approx4.6\times10^{15}$ photons s^{-1} cm^{-2} over a large volume (60 ml).

Transient absorption experiments in the 20 ns to 500 μs region were carried out on a nanosecond laser flash photolysis spectrometer from Applied Photophysics (LKS 60). The laser excitation at 355 nm from Quanta Ray GCR 130-1 Nd: YAG (pulse width ≈9 ns) was used in a right angle geometry with respect to the monitoring light beam. The transient absorbances at preselected wavelengths were monitored by a detection system consisting of a pulsed Xenon lamp (150 W), monochromator and a 1P28 photomultiplier. A spectrometer control unit was used for synchronizing the pulse light source and programmable shutters with the laser output. It also housed the high voltage power supply for the photomultiplier. The signal from the photomultiplier was digitized by a programmable digital oscilloscope (HP54522A). A 32 bit RISC-processor kinetic spectrometer workstation was used to analyse the digitized signal.

2.3. Analysis

Fe(II) concentration was determined by complexometry with *o*-phenanthroline, using $\varepsilon_{510}=1.118\times10^4$ l mol^{-1} cm^{-1} for the Fe(II)–phenanthroline complex [17].

The monomeric concentration of Fe(III), i.e. $[Fe(OH)]^{2+}$, was determined by using the modified Kuenzi's procedure [18] and which was described earlier [15].

The quantum yield of 4-OP degradation as well as the kinetics of the photoproducts formation were determined by high performance liquid chromatography experiments ($\lambda_{detection}=224$ nm).

3. Results and discussion

3.1. Characterisation of the mixture 4-OP/Fe(III)

The work was performed on the commercial 4-OP product used for the synthesis of octylphenol polyethoxylates

(IGEPAL CA 520) studied in our recent work [15]. Its chemical structure was determined by ^{1}H NMR spectroscopy.

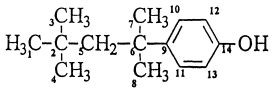

^{1}H (CD_3CN, δ): 7.2 (d, 2H, H_{12} and H_{13}); 6.7 (d, 2H, H_{10} and H_{11}); 1.7 (s, 2H, H_5); 1.3 (s, 6H, H_7 and H_8); 0.7 (s, 9H, H_1 and H_4).

The branched alkyl chain, which is the hydrophobic moiety of 4-OP, explains the low solubility of this compound in aqueous solution [19]. The maximum solubility was determined to be ca. 4.8×10^{-5} mol l^{-1} at room temperature. For the degradation study of 4-OP a more concentrated solution was necessary. This was obtained by working with 5% of acetonitrile in the mixture 4-OP/Fe(III). Under these conditions, the maximum solubility of 4-OP was determined to be equal to 1.3×10^{-4} mol l^{-1} which allowed us to carry out in a convenient manner the identification of the photoproducts formed during 4-OP degradation.

4-OP absorbs in the ultraviolet region with two maxima at 222 nm (ε=7700 l mol^{-1} cm^{-1}) and 277 nm (ε=1700 l mol^{-1} cm^{-1}).

Under our experimental conditions (3.0×10^{-4} mol l^{-1} and pH=3.5), $Fe(OH)^{2+}$ is the predominant monomeric Fe(III)–hydroxy complex [11]. However, the concentration of monomeric species rapidly decreased after dissolution of ferric perchlorate in water. The disappearance was attributed to the possible formation of soluble aggregates [20]. It clearly appeared that the percentage of $Fe(OH)^{2+}$ strongly depended on the age of the ferric solution and on the starting concentration [11]. By using the HQSA method, the percentage of $Fe(OH)^{2+}$ in solution was determined according to the following expression:

$$\%Fe(OH)^{2+} = \frac{[Fe(OH)^{2+}]}{[Fe(III)]_{tot}} \times 100$$

$[Fe(III)]_{tot}$ is the concentration of total dissolved Fe(III).

The disappearance of the monomeric species was slightly accelerated by the presence of 5% of acetonitrile in water (Fig. 1). This phenomenon could be explained by the complexation between Fe(III) and acetonitrile; it was detected by UV–VIS spectrophotometry at higher percentage of acetonitrile, but quantitative analysis failed due to the extreme complexity of the system. The different percentages of $Fe(OH)^{2+}$ were obtained by the use of Fe(III) solutions of different ages.

The mixture of 4-OP/Fe(III) in our experimental conditions was thermally stable (in the dark and at room temperature) in terms of 4-OP concentration. The resulting UV–VIS spectrum was the sum of the spectra of the two components. Thus, no detectable interaction in the ground state was observed.

Unless particular indications, the following standard experimental conditions were used: Fe(III) (3.0×10^{-4} mol l^{-1}, ≈80% of monomeric species)/4-OP (1.0×10^{-4} mol l^{-1}) in water with 5% of acetonitrile.

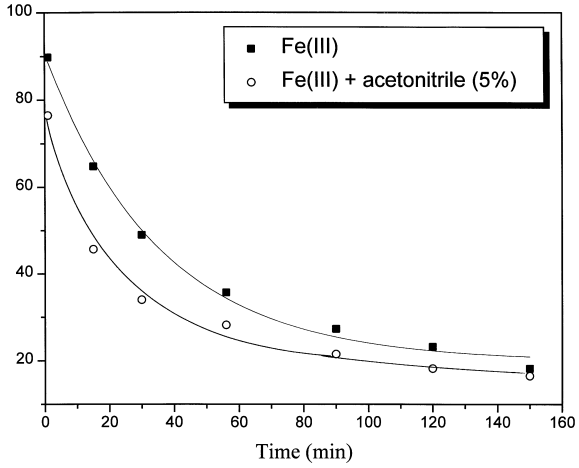

Fig. 1. Disappearance of Fe(III) monomeric species in the absence and in the presence of acetonitrile.

3.2. Photochemical behaviour

Upon continuous irradiation the formation of Fe(II) was followed by complexometry. Fe(II) concentration quickly rose, then reached a constant value (Fig. 2). A limit value was also observed on the disappearance kinetics of $Fe(OH)^{2+}$. This plateau has to be related to the reoxidation of Fe(II) into Fe(III) monomeric species. This point is of great interest since $Fe(OH)^{2+}$ is the most photoactive species. It has to be pointed out that the limit value of the Fe(II) concentration increased by increasing $Fe(OH)^{2+}$ concentration, as already mentioned for similar systems [12].

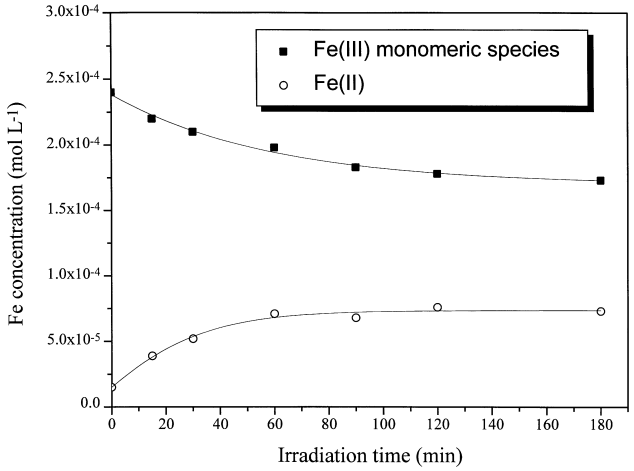

Fig. 2. Kinetics of Fe(II) formation and Fe(III) monomeric species disappearance during irradiation at 365 nm of a mixture of 4-OP (1.0×10^{-4} mol l^{-1}) and Fe(III) (3.0×10^{-4} mol l^{-1}; 80% of monomeric species).

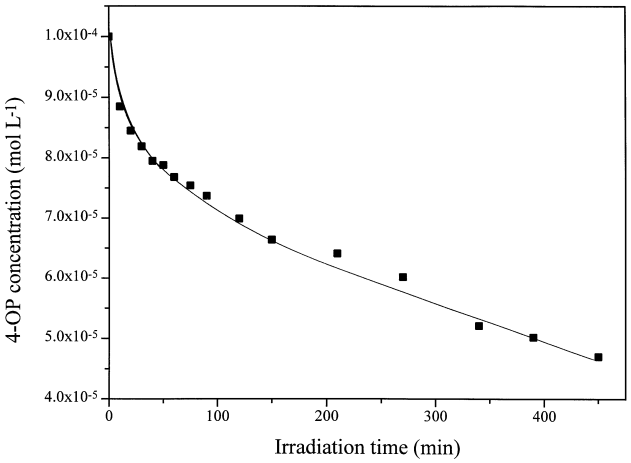

Fig. 3. Kinetic of 4-OP disappearance during irradiation at 365 nm of a mixture of 4-OP (1.0×10^{-4} mol l^{-1}) and Fe(III) (3.0×10^{-4} mol l^{-1}; 90% of monomeric species).

3.2.1. 4-OP disappearance

Upon irradiation at 365 nm, the concentration of 4-OP continuously decreased (Fig. 3). The disappearance showed two distinct domains; for short irradiation times, the disappearance of 4-OP was very fast, then the degradation of 4-OP slowed down after ca. 50 min. The degradation of 4-OP continues because of the regeneration of Fe(III) monomeric species in the solution.

3.2.2. Influence of $Fe(OH)^{2+}$ concentration

In this set of experiments, the percentage of $Fe(OH)^{2+}$ species was taken as 92, 79, 47 and 28%. The values of the initial quantum yield of 4-OP disappearance at 365 nm are gathered in Table 1. They show that the rate of 4-OP disappearance increased when the percentage of the monomeric species of iron(III) in the solution increased.

3.2.3. Influence of the irradiation wavelength

The initial quantum yield of 4-OP disappearance was also determined at different excitation wavelengths present in the solar emission (365, 334, 313 and 296 nm). The results, which are summarised in Table 2, show that the degradation of 4-OP is more efficient when the irradiation was carried out with high energy light. This phenomenon is very often observed with Fe(III) salts [12,15].

Table 1
Influence of the Fe(III) monomeric species concentration on the initial quantum yield of 4-OP disappearance

Percentage of $Fe(OH)^{2+}$	$\Phi_{\text{4-OP disappearance}}$
28	0.003
47	0.004
79	0.006
92	0.010

Table 2
Influence of the irradiation wavelength on the initial quantum yield of 4-OP disappearance

$\lambda_{exc.}$ (nm)	$\Phi_{\text{4-OP disappearance}}$
296	0.014
313	0.011
334	0.010
365	0.006

Table 3
Influence of the 4-OP concentration on the initial quantum yield of 4-OP disappearance

[4-OP] (mol l^{-1})	$\Phi_{\text{4-OP disappearance}}$
1.0×10^{-4}	0.0061
5.0×10^{-5}	0.0033
1.0×10^{-5}	0.0005

3.2.4. Influence of the 4-OP concentration

The effect of 4-OP concentration was investigated within the range 1.0×10^{-5}–1.0×10^{-4} mol l^{-1} and under excitation at 365 nm. The concentration range was controlled by the UV–VIS detector (lower limit) and the solubility of 4-OP (upper limit). The results collected in Table 3 show that the quantum yield of 4-OP disappearance increases with the starting 4-OP concentration.

3.2.5. 2-Propanol effect

In the presence of 2% of 2-propanol, a radical scavenger, the degradation of 4-OP upon irradiation at 365 nm is totally inhibited.

3.3. Photoproducts identification

Fig. 4 shows a relatively complex HPLC chromatogram of an irradiated mixture (4-OP/iron(III)) at 365 nm. Photo-

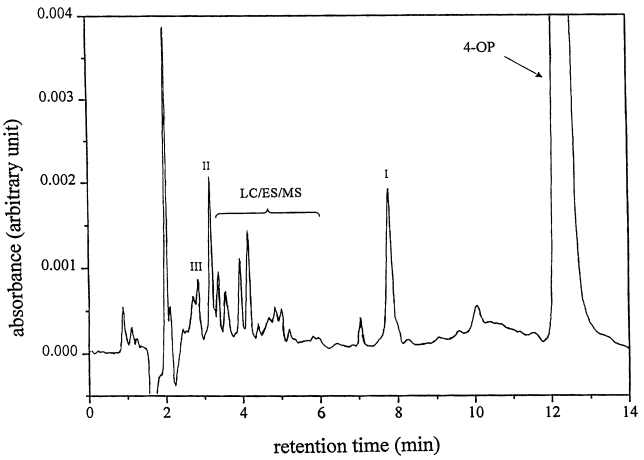

Fig. 4. HPLC chromatogram of a mixture of 4-OP (1.0×10^{-4} mol l^{-1}) and Fe(III) (3.0×10^{-4} mol l^{-1}; 80% of monomeric species) irradiated 60 min at 365 nm. Detection: λ=224 nm. Eluent: acetonitrile/water (75/25 v/v).

products more polar than the starting substrate appeared; some of them have been identified.

Photoproduct (I) has been separated by preparative HPLC and analysed by ^{1}H NMR spectroscopy. The result is in agreement with the chemical structure of 4-(1,1,3,3-tetramethylbutyl)pyrocatechol (4-OPC):

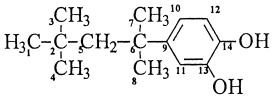

^{1}H (CD_3CN, δ): 6.85 (d, H_{11}, J=2 Hz with H_{10}); 6.7 (dd, H_{10}, J=2 Hz with H_{11} and J=8 Hz with H_{12}); 6.65 (d, H_{12}, J=8 Hz with H_{10}); 1.7 (s, 2H, H_5) 1.3 (s, 6H, H_7 and H_8); 0.7 (s, 9H, H_1, H_3 and H_4).

This identification has been confirmed by LC/ES/MS analysis which gave m/z=222 for the molecular peak and m/z=151 for the major fragment.

The UV–VIS spectrum of 4-OPC presents two maxima near 265 and 395 nm. The difference with the UV–VIS spectrum of 4-OP (222 and 277 nm) can not be explained by the additional hydroxyl radical on the aromatic ring. We have suggested that the absorption at 395 nm could be a consequence of a complexation between Fe(III) and 4-OPC as already stated with diphenols [21]. The addition of Fe(III) into a solution of catechol leads to the appearance of a similar maximum at 395 nm. The kinetics of 4-OPC formation and disappearance is represented in Fig. 5. The maximum

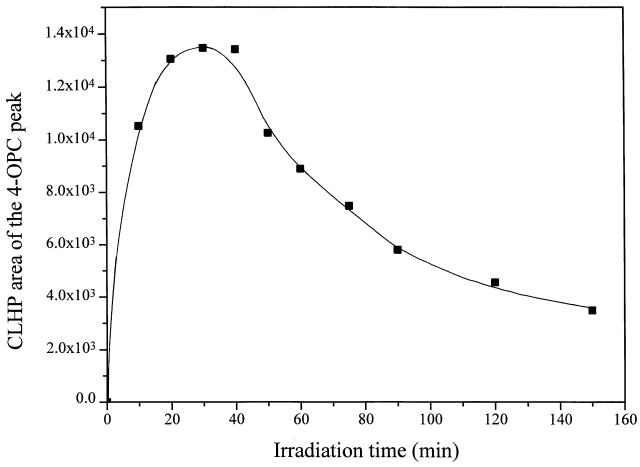

Fig. 5. Kinetic of 4-OPC formation and disappearance during irradiation at 365 nm of a mixture of 4-OP (1.0×10^{-4} mol l^{-1}) and Fe(III) (3.0×10^{-4} mol l^{-1}; 90% of monomeric species).

of formation was reached in the early stages of the reaction (it accounts for ≈10% of 4-OP disappearance) then the concentration rapidly decreased due more likely to a its direct excitation. Such a behavior was not observed for the other photoproducts, which accumulated in the solution.

Benzoquinone(II) and 4-hydroxyacetophenone(III) were identified as photoproducts by comparison with the authentic samples. All identified photoproducts are gathered in Table 4. The photoproducts (IV–VII) were identified by

Table 4
Chemical structures of the photoproducts identified

	Chemical structures	Identification	m/z Molecular peak, major fragment
I	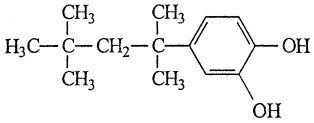	LC/ES/MS	222, 151
II	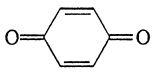	Authentic sample	
III	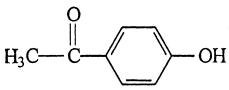	Authentic sample	
IV	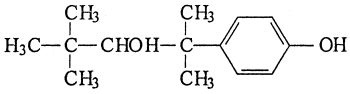	LC/ES/MS	222, 135
V	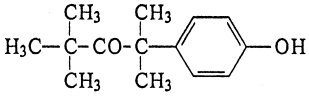	LC/ES/MS	220, 135
VI	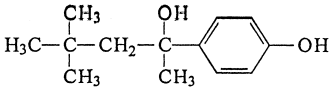	LC/ES/MS	208, 190
VII	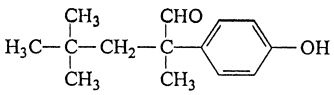	LC/ES/MS	220, 149

HPLC/ES/MS; they only come from the oxidation on different sites of 4-OP alkyl chain. All the attempts to detect any formation of dimeric photoproducts failed.

In the absence of oxygen, the formation of 4-OPC significantly increased while that of the oxidation photoproducts on the alkyl chain decreased. In the meantime no significant difference was observed on the rate of 4-OP disappearance.

3.4. Mechanism and discussion

3.4.1. Laser flash photolysis experiments

In order to establish the primary mechanism of the degradation and the nature of the implicated transient species, fast kinetic study was realised. In this set of experiments, it was necessary to work at concentrations higher than those used for the steady state studies: [Fe(III)]=2.0×10^{-3} mol l^{-1}, [4-OP]=6.0×10^{-4} mol l^{-1} in water/acetonitrile (8/2 by volume). Fresh solutions of Iron(III) were used to insure that the percentage of $Fe(OH)^{2+}$, the more photoactive species, was between 100 and 85%.

Laser flash photolysis of the solution Fe(III)/4-OP at 355 nm resulted in the immediate appearance of an absorption within the range 380–400 nm. The transient spectrum shows an absorption maximum around 415 nm and a shoulder at 400 nm (Fig. 6). The similarity of this spectrum with those reported for phenoxyl radicals [22] let us suspect the instantaneous formation of 4-octylphenoxyl radical. Support for this hypothesis comes from the experiments with $[Co(NH_3)_5N_3]^{2+}$. Under excitation into the charge transfer band (LMCT) of this cobalt complex, a photoredox process leading to the formation of the azide radical, $N_3^\bullet$, is present. $N_3^\bullet$ reacts quantitatively and selectively with phenol derivatives by electron transfer process giving rise to the formation of the corresponding phenoxyl radical [23–25]. The laser experiments undertaken at 355 nm with the system $[Co(NH_3)_5N_3]^{2+}$/4-OP gave an absorption spectrum similar to that obtained by excitation of Fe(III)/4-OP solution (Fig. 6). The formation of 4-octylphenoxyl radical can then be explained by the following process:

$$[Co(NH_3)_5N_3]^{2+} \xrightarrow{LMCT} Co(II) + N_3^\bullet + 5NH_3$$

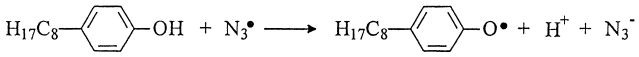

In the presence of Fe(III), the rate of formation of 4-octylphenoxyl radical was studied with two different starting concentrations of 4-OP, 6.0×10^{-4} and 2.0×10^{-4} M, on the time scale of 5 μs (Fig. 7). The formation followed a first order kinetic and was independent on the initial concentration of 4-octylphenol. This leads to the conclusion that 4-octylphenoxyl radical is mainly formed *via* a unimolecular process with a rate constant of 1.5×10^{6} s^{-1}. Its disappearance showed a second order kinetics with $k/\varepsilon_{415\,nm}=1.8\times10^{7}$ cm s^{-1}.

In the absence of 4-OP, the trace obtained under laser flash photolysis and by detection below 380 nm showed an important and constant bleaching due to the photoreduction of Fe(III) into Fe(II). In the presence of 4-OP, in addition to the bleaching the analysis at 350 nm gave evidence for the formation of a second intermediate. Its rate of formation was three times higher than that of 4-phenoxyl radical.

3.4.2. Mechanism

As already reported in the literature and in our earlier work in pure water [11–13], the photolysis of Fe(III) aquo-complexes and more particularly $Fe(OH)^{2+}$ leads to the following process.

$$Fe(OH)^{2+} \xrightarrow{h\nu} Fe^{2+} + {}^\bullet OH$$

However, taking into account the present experimental conditions, i.e. 5% acetonitrile in steady state studies and 20%

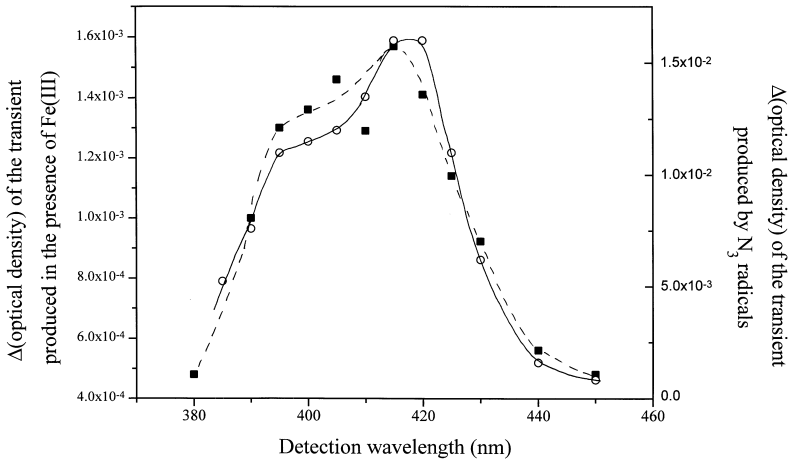

Fig. 6. UV–VIS spectra of the transients produced during the irradiation at 355 nm of a solution of 4-OP (6.0×10^{-4} mol l^{-1}; acetonitrile 20%): (■) represents in the presence of Fe(III); (○) represents in the presence of $[Co(NH_3)_5N_3]^{2+}$.

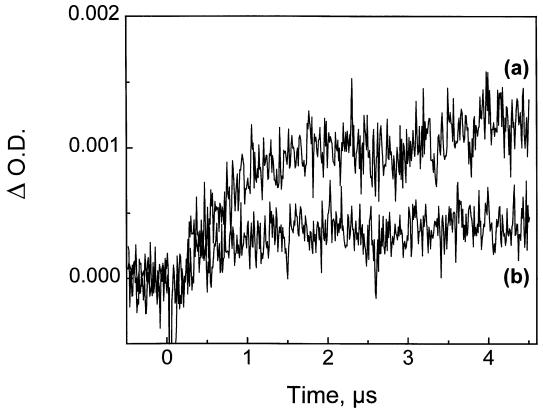

Fig. 7. Trace observed at 415 nm following laser photolysis (355 nm) in water/acetonitrile solution (8/2 by volume). (a) 4-OP 6.0×10^{-4} mol l^{-1} and Fe(III) 2.0×10^{-3} mol l^{-1}; (b) 4-OP 2.0×10^{-4} mol l^{-1} and Fe(III) 2.0×10^{-3} mol l^{-1}.

in laser flash photolysis experiments, one can no longer attribute the total degradation of 4-octylphenol to the action of hydroxyl radicals. In the presence of acetonitrile the latter radicals mainly disappears leading to $^{\bullet}CH_2CN$ (k ($^{\bullet}OH+CH_3CN$)$=2.2\times10^7$ mol^{-1} l s^{-1} [26]).

Under laser flash photolysis, the formation of 4-octylphenoxyl radical was clearly established with a rate independent on the starting concentration of 4-octylphenol. This argues against a significant involvement of acetonitrile derived radical or acetonitrile peroxyl radical (in the presence of oxygen) in the process. On the basis of the above experimental results, one may conceive that an interaction of 4-octylphenol and Fe(III) in its excited state is involved which undergoes an electron transfer process with the formation of 4-octylphenoxyl radical. The following initial processes may then be proposed:

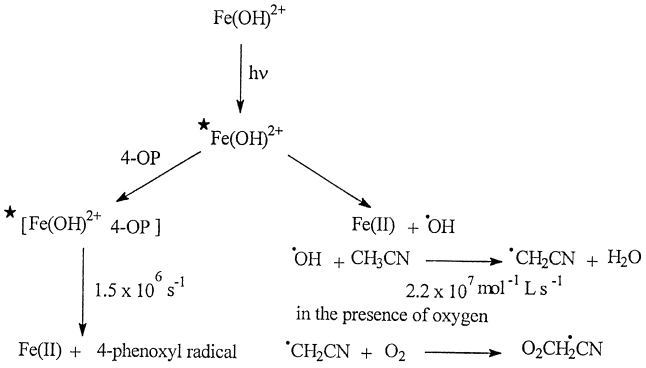

This scheme accounts for the dependence of the 4-octylphenol quantum yield disappearance on the initial concentration of 4-OP. The quenching pathway is favoured when the substrate concentration increased. No assignment is given for the transient observed at 350 nm. Since hydroxyl radical is totally consumed by the reaction with acetonitrile, it can not be attributed to the adduct generally formed by action of $^{\bullet}OH$ and 4-octylphenol.

The phenoxyl radical is oxidized by Fe(III) to the alkoxyl radicals (3) and (4) [12]. This reaction of Fe(III) on the phenoxyl radical can explain that no dimer products were found: the concentration in phenoxyl radicals being too low to permit the formation of dimer.

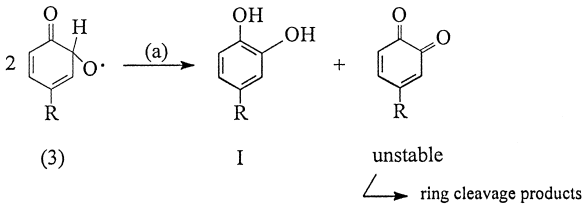

The alkoxyl radical (3) can react by disproportionation giving rise to the formation of 4-OPC (photoproduct I) (reaction a). Similar reaction was described for hydroquinone [28].

The scission of the alkoxyl radical (4) could lead to the formation of benzoquinone (photoproduct II) (reaction b).

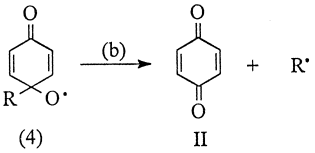

The attack of acetonitrile derived peroxyl radicals, by hydrogen abstraction, on the alkyl chain [27] leads to the radicals $R_1^{\bullet}$ and $R_2^{\bullet}$ which can react with oxygen to form two peroxyl radicals $R_1O_2^{\bullet}$ and $R_2O_2^{\bullet}$.

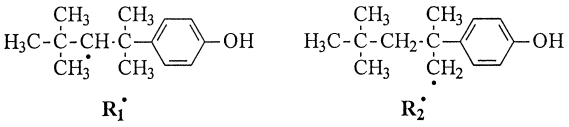

The peroxyl radicals $R_1O_2^{\bullet}$ and $R_2O_2^{\bullet}$ can undergo a head-to-head termination reaction to form intermediate tetroxides. The different ways of decomposition of these intermediates were described by Von Sonntag and Schuchmann [27]. $R_1^{\bullet}$ leads to the formation of the alcohol (IV) and the ketone (V). $R_2^{\bullet}$ leads directly to the formation of aldehyde (VII). 4-hydroxyacetophenone (III) and alcohol in α position of aromatic ring (VI) are also formed from $R_2^{\bullet}$ but by a two step process.

The different ways of decomposition allow to explain the formation of all the identified primary photoproducts. The photoproducts (III, IV, V, VI and VII) imply reaction with oxygen, confirming their important decrease in the absence of oxygen.

4. Conclusion

The degradation of 4-OP degradation mainly involves two pathways (i) formation of acetonitrile derived radical and acetonitrile peroxyl radical (in the presence of oxygen) *via* the formation of hydroxyl radical and (ii) an interaction

with Fe(III) in the excited state. This latter process leads to the formation of the 4-octylphenoxyl radical by electron transfer reaction.

Acknowledgements

The authors indebted to the anonymous reviewer for his helpful comments and suggestions.

References

[1] R. Renner, Environ. Sci. Technol. 31 (1997) 316A.
[2] Y. Fujita, M. Reinhard, Environ. Sci. Technol. 31 (1997) 1518.
[3] W. Giger, P.H. Brunner, C. Shaffner, Science 225 (1984) 623.
[4] M. Ahel, W. Giger, Anal. Chem. 57 (1985) 1577.
[5] A. Di Corcia, C. Crescenzi, A. Marcomini, R. Samperi, Environ. Sci. Technol. 32 (1998) 711.
[6] D.W. Mc Leese, V. Zitko, C.D. Metcalfe, D.B. Sergeant, Chemosphere 9 (1980) 79.
[7] S.L. Andrianirinaharivelo, J-F. Pilichowski, M. Bolte, Trans. Met. Chem. 18 (1993) 37.
[8] F.K. Günter, S. Hilger, S. Canonica, Environ. Sci. Technol. 29 (1995) 1008.
[9] E. Matthijs, N.T. De Oude, M. Bolte, J. Lemaire, Water Res. 23 (7) (1989) 845.
[10] F.S. Dainton, M. Tordoff, Trans. Faraday Soc. 53 (1957) 666.
[11] B.C. Faust, J. Hoigné, Atmos. Environ. 24A (1990) 79.
[12] P. Mazellier, G. Mailhot, M. Bolte, New J. Chem. 21 (1997) 389.
[13] N. Brand, G. Mailhot, M. Bolte, Chemosphere 34 (12) (1997) 2637.
[14] G. Mailhot, M. Astruc, M. Bolte, Appl. Organomet. Chem. 13 (1999) 53.
[15] N. Brand, G. Mailhot, M. Bolte, Environ. Sci. Technol. 32 (1998) 2715.
[16] M. Linhard, H. Flygare, Z. Inorg. Chem. 262 (1950) 328.
[17] J.G. Calvert, J.M. Pitts, Photochemistry, Wiley, New York, 1966, 783 pp.
[18] W.H. Kuenzi, Die Hydrolyse von Eisen(III) der Enfluss von Chlorid auf Bildung und Zerfall von Vernetzungsprodukten Ph.D. dissertation ETH no. 7016, Eidgenössischem Technischem Hochschule, Zurich, Switzerland, 1982.
[19] M. Ahel, W. Giger, Chemosphere 26 (8) (1993) 1461.
[20] C.M. Flynn, Chem. Rev. 84 (1) (1984) 31.
[21] V. Grignard, Traité de Chimie Organique, Masson, Paris, 1940, 781 pp.
[22] R. Terzian, N. Serpone, M.A. Fox, J. Photochem. Photobiol. A: Chem. 90 (1995) 125.
[23] M. Sarakha, H. Burrows, M. Bolte, J. Photochem. Photobiol. A: Chem. 97 (1996) 81.
[24] M. Sarakha, M. Bolte, J. Photochem. Photobiol. A: Chem. 97 (1996) 87.
[25] U. Stafford, K.A. Gray, P.V. Kamat, J. Phys. Chem. 98 (1994) 6343.
[26] G.V. Buxton, C.L. Greenstock, W.P. Helman, A.B. Ross, J. Phys. Chem. Ref. Data 17 (1988) 513.
[27] C. von Sonntag, H-P. Schuchmann, Angew. Chem. Int. Ed. Engl. 30 (1991) 1229.
[28] P. Boule, A. Rossi, J.-F. Pilichowski, G. Grabner, New J. Chem. 16 (1992) 1053.